Stoichiometry for binding and transport by the twin arginine translocation system

Jose M. Celedon and Kenneth Cline

Horticultural Sciences Department and Plant Molecular and Cellular Biology, University of Florida, Gainesville, FL 32611

Twin arginine translocation (Tat) systems transport large folded proteins across sealed membranes. Tat systems accomplish this feat with three membrane components organized in two complexes. In thylakoid membranes, cpTatC and Hcf106 comprise a large receptor complex containing an estimated eight cpTatC-Hcf106 pairs. Protein transport occurs when Tha4 joins the receptor complex as an oligomer of uncertain size that is thought to form the protein-conducting structure. Here, binding analyses with intact membranes or purified complexes indicate that each receptor complex could bind eight precursor proteins. Kinetic analysis of translocation showed that each precursor-bound site was independently functional for transport, and, with sufficient Tha4, all sites were concurrently active for transport. Tha4 titration determined that ~26 Tha4 protomers were required for transport of each OE17 (oxygen-evolving complex subunit of 17 kD) precursor protein. Our results suggest that, when fully saturated with precursor proteins and Tha4, the Tat translocase is an ~2.2-megadalton complex that can individually transport eight precursor proteins or cooperatively transport multimeric precursors.

Introduction

The Tat (twin arginine translocation) system transports folded proteins across ion-tight membranes using the proton-motive force as the sole energy source (Berks et al., 2000; Müller and Klösgen, 2005; Lee et al., 2006; Cline and Theg, 2007). These unusual features differentiate Tat from most other protein translocation systems, which transport proteins in an unfolded conformation and are powered by nucleoside triphosphate hydrolysis. Tat systems transport substrates that vary in size from ~2 kD to >100 kD, meaning that the Tat protein–conducting structure has the ability to adjust its opening according to the passenger protein (Berks et al., 2000). Moreover, it must do this in a way that precludes uncontrolled ion (proton) leakage. Tat can also transport precursor proteins that form oligomers. This can happen when all subunits have signal peptides and are bound to the same Tat receptor complex (Ma and Cline, 2010) or when only one subunit has a signal peptide and another subunit hitchhikes across the membrane (Rodrigue et al., 1999; Berks et al., 2000).

These remarkable feats are accomplished with only three membrane protein components: cpTatC, Hcf106, and Tha4 in thylakoids and the orthologous TatC, TatB, and TatA in prokaryotes. The components are found in two separate complexes in the membrane. cpTatC and Hcf106 form a large receptor complex (Cline and Mori, 2001). Site-directed cross-linking studies identified cpTatC (TatC) as the primary receptor for the twin arginine signal peptide (Alami et al., 2003; Gérard and Cline, 2006). The receptor complex has been characterized in detergent extracts as a heterooligomer of 500–700 kD that contains only cpTatC-Hcf106 (TatC-TatB) in a 1:1 molar ratio (Bolhuis et al., 2001; Cline and Mori, 2001; McDevitt et al., 2006). This and other considerations (see Discussion) suggest approximately eight copies of each component per complex. The estimated number of cpTatC-Hcf106 pairs per complex suggests that each receptor complex could potentially bind approximately eight precursor proteins. However, this question is currently unresolved. Single-particle electron microscopic analysis of purified *Escherichia coli* receptor complexes showed a maximum of two precursor proteins per complex (Tarry et al., 2009). In contrast, Ma and Cline (2010) showed evidence for at least four precursors bound to an individual receptor complex.

Correspondence to Kenneth Cline: kcline@ufl.edu

J.M. Celedon's present address is Michael Smith Laboratories, University of British Columbia, Vancouver, BC V6T 1Z4, Canada.

Abbreviations used in this paper: IB, import buffer; IVT, in vitro translated; WG, wheat germ.

Supplemental material can be found at:
http://doi.org/10.1083/jcb.201201096

The Rockefeller University Press $30.00
J. Cell Biol. Vol. 197 No. 4 523–534
www.jcb.org/cgi/doi/10.1083/jcb.201201096

Table 1. **Reevaluation of Tat components in pea chloroplasts and thylakoids**

Protein	Intact chloroplasts (molecule/cp)		Thylakoids (molecule/thylakoid)		Stoichiometry	
	Mean	SD	Mean	SD	Chloroplasts	Thylakoids
cpTatC	8,800	400	9,700	200	1	1
Hcf106	39,000	2,000	37,700	1,800	~4	~4
Tha4	186,500	12,900	127,900	31,700	~21	~13

The molecules of cpTat components per chloroplast and thylakoid were determined by quantitative immunoblotting using full-length IVT protein standards (see Materials and methods, Fig. S1, and Tables S1 and S2) and are the means and SDs of three biological replicates. Chloroplasts and washed thylakoids were isolated from pea seedlings (see Materials and methods).

Binding of the precursor protein to the receptor complex triggers assembly of Tha4 homooligomers to form a transient translocase complex (Mori and Cline, 2002). Tha4 likely facilitates some kind of passageway across the lipid bilayer, possibly by forming a transient or gated channel. In this context, the size of the Tha4 oligomer in the translocase is likely to reflect the dimensions of the substrate to be transported. However, current knowledge about the organization of the Tha4 (TatA) oligomer in the translocase is ambiguous. TatA was initially thought to exist as a collection of large homooligomers (Gohlke et al., 2005), and it was suggested that oligomers were selectively recruited to fit the size of the folded substrate (Sargent et al., 2006). However, two recent studies indicate that Tha4 (TatA) exists as tetramers in inactive membranes and only forms larger oligomers upon assembling with the receptor complex in transporting membranes (Leake et al., 2008; Dabney-Smith and Cline, 2009). Both studies provide support for a polymerization model wherein docking of tetrameric Tha4 (TatA) with an occupied receptor site induces Tha4 (TatA) polymerization until the oligomer is sufficient to support transport. Unfortunately, the transient existence of the translocase has made determining the size of the transport-active oligomer very difficult.

The aforementioned considerations underscore the fact that an accurate measure of the stoichiometry of precursor proteins and Tat components in the binding and transport reactions is key to understanding the mechanisms involved. Here, we used quantitative biochemical analyses as well as analysis of transport kinetics toward that goal. Our results indicate that each cpTatC subunit can bind a precursor protein, implying that each receptor complex can bind approximately eight precursor proteins (see Discussion). We find no evidence of cooperativity between binding sites, suggesting that each site binds a precursor protein independently. Kinetic analysis of the translocation of bound precursor proteins with varying receptor occupancy levels leads us to postulate that, when Tha4 is in excess, all sites are capable of transporting their bound precursor proteins independently of other sites. By titrating Tha4, we estimated that ~26 Tha4 are necessary to activate a tOE17-bound site for transport. These results can be interpreted to mean that a minimal translocase unit for OE17 (oxygen-evolving complex subunit of 17 kD) transport is 1 cpTatC (1 Hcf106) and 26 Tha4. Moreover, they portray a unique multivalent protein translocase that can transport up to eight precursor proteins individually or, under certain conditions, cooperatively transport multimeric precursor proteins (Ma and Cline, 2010).

Results

Methodology

The tOE17 V-20F precursor protein is an OE17 precursor modified with a phenylalanine at the twin arginine (RR) +2 position, resulting in higher affinity binding (Ma and Cline, 2000; Gérard and Cline, 2007). The RR +2F motif is found in at least one cpTat substrate (Summer et al., 2000) and most bacterial Tat substrates, where it plays an important role in transport efficiency (Stanley et al., 2000). The binding affinity of tOE17 V-20F, although greater than most cpTat substrates, allowed analysis of binding stoichiometry with intact membranes and with in vitro translated (IVT) precursor protein, which exhibits a very low level of nonspecific binding (Ma and Cline, 2000). In the figures and discussion that follow, this precursor will be referred to as tOE17 or RR-tOE17. A nonfunctional twin lysine variant of this precursor is referred to as KK-tOE17.

Accurate quantification of tOE17 and cpTat components was crucial to this study. IVT proteins were quantified by scintillation counting, with appropriate corrections for the specific radioactivity of the tracer amino acid in the translation reaction (Fig. S1) and recovery of proteins from gel slices (see Materials and methods; Table S1). A novel and accurate immunoblotting method was developed to quantify cpTat components. It uses full-length IVT proteins as immunoblot standards (Fig. S1 and Table S2). Previous studies using aqueous soluble peptide antigens as immunoblotting standards reported a relatively low ratio of Tha4 to cpTatC (Mori et al., 2001; Jakob et al., 2009). We found that peptide standards dramatically overestimate cpTatC (Fig. S2) and thus underestimate the Tha4 per cpTatC stoichiometry. Our improved method produced a revised stoichiometry of 21:1 for Tha4/cpTatC in pea chloroplasts and somewhat less in washed thylakoids (Table 1), which supports the proposed role of Tha4 (TatA) as a channel component and further supports conclusions that Tha4 is easily removed from thylakoids during isolation and buffer washes (Frielingsdorf et al., 2008).

Precursor proteins bind to the Tat receptor with rapid association and a very low rate of dissociation

Relative rates of association and dissociation of tOE17 were determined before analysis of binding stoichiometry. Binding of tOE17 to the receptor complex occurred faster than we could practically determine with our assay, i.e., <5 min. Because binding reactions were performed for 60 min, equilibrium was assured even with low concentrations of tOE17. Dissociation of

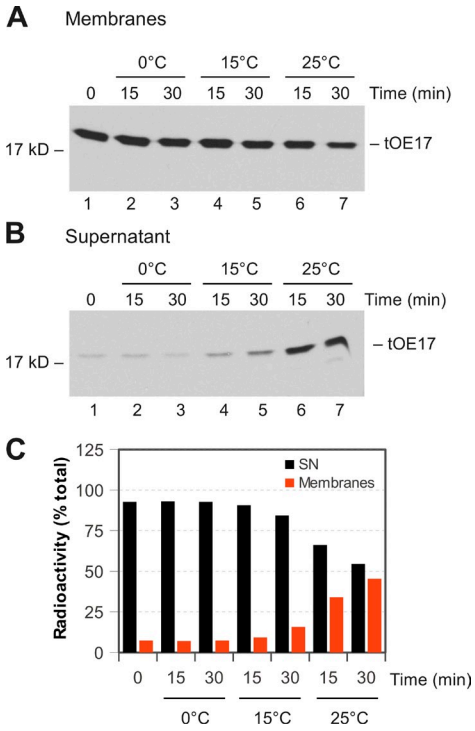

Figure 1. **The tOE17 precursor binds to the receptor complex with high affinity and a low rate of dissociation.** (A and B) Thylakoid membranes were incubated with saturating amounts of radiolabeled tOE17, as determined in Fig. 3. Membranes were then recovered, washed twice, and incubated with saturating amounts of unlabeled tOE17 at 0, 15, or 25°C. At time points, aliquots were removed, and the membrane (A) and supernatant (B) fractions were analyzed by SDS-PAGE and fluorography. (C) Radioactivity was measured by scintillation counting of extracted gel slices and plotted as a percentage of the total for each time point. The data are from a single experiment, which is representative of several similar experiments conducted at the temperatures shown. SN, supernatant.

membrane-bound tOE17 was tested with thylakoids saturated with radiolabeled tOE17 and then incubated with saturating amounts of unlabeled tOE17. Under these conditions, any radiolabeled tOE17 that dissociated from its binding site would be replaced by unlabeled tOE17. As can be seen in Fig. 1, the amount of radiolabeled tOE17 recovered after 30 min at 0°C (lane 3 in Fig. 1 [A and B]) was essentially the same as the 0 time control (lane 1 in Fig. 1 [A and B]), i.e., no dissociation at 0°C. Dissociation at 15°C was 3 and 9% at 15 and 30 min, respectively (lanes 4 and 5 in Fig. 1 [A and B]). A substantial percentage of radiolabeled tOE17 was released to the supernatant only when the incubation temperature was increased to 25°C. Because binding and receptor complex purification experiments were conducted at 0–4°C and transport reactions at 15°C, only minor amounts of tOE17 would conceivably dissociate from the binding site during these procedures.

Nonspecific binding

Binding specificity was examined in several ways: binding of the nonfunctional twin lysine precursor protein KK-tOE17, binding to thylakoids pretreated with antibodies to cpTat receptor components, and binding to membranes pretreated with protease. Binding reactions were conducted with concentrations of precursor protein that would saturate the binding sites.

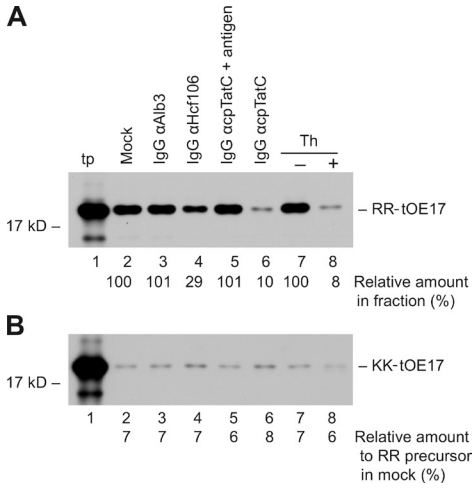

Figure 2. **The tOE17 precursor binds directly and specifically to cpTatC.** (A and B) Thylakoid membranes were treated with 0.5 mg/ml IgGs (lanes 3–6) in the absence or presence of ~4 µM antigen (lane 5) for 1 h on ice and then incubated with saturating amounts (determined in Fig. 3) of radiolabeled RR-tOE17 (A, translation product [tp] lane 1) or nonfunctional KK-tOE17 (B, tp lane 1). Alternatively, thylakoids were treated or mock treated with 100 µg/ml thermolysin (Th; lanes 7 and 8) for 40 min on ice. Proteolysis was terminated with EDTA, after which membranes were recovered, washed with IB 5 mM EDTA, resuspended in IBM, and then incubated with saturating amounts of RR-tOE17 (A) or KK-tOE17 (B) for 60 min. Membranes were recovered, washed, and analyzed (see Materials and methods).

As shown in Fig. 2 A, pretreatment with antibodies to cpTatC, the primary receptor component (Alami et al., 2003; Gérard and Cline, 2006), reduced precursor protein binding to ~10% of that with mock-treated membranes (Fig. 2 A, lane 6). This reduction did not occur if the cpTatC antigen was included in the antibody-binding reaction (Fig. 2 A, lane 5). Similarly, protease pretreatment of the membranes reduced binding to ~8% of mock-treated membranes (Fig. 2 A, lanes 7 and 8). Consistent with these values, binding of the nonfunctional KK-tOE17 was ~7% of RR-tOE17 binding and was unaffected by antibody or protease pretreatment (Fig. 2 B, lanes 2–8). Thus, with the conditions used to measure binding in this study, a low percentage of RR-tOE17 binds nonspecifically to the lipid bilayer. Furthermore, binding of KK-tOE17 is a representative measure for nonspecific binding.

Stoichiometry of tOE17 per cpTatC determined from saturation-binding isotherms

Saturation binding experiments were performed as a first approach to determine precursor protein binding stoichiometry to cpTatC. Thylakoids recovered from each binding reaction were analyzed by SDS-PAGE/fluorography to quantify tOE17 (Fig. 3 A) and SDS-PAGE/immunoblotting to quantify cpTatC (e.g., see Fig. S1 and Materials and methods). The expected binding saturation curve was obtained but with gradually increased binding at higher tOE17 concentrations (Fig. 3 C). Nonspecific binding, estimated with KK-tOE17 (Fig. 3, B and C), was linear in the concentration range used in the assay. Subtracting nonspecific binding at each concentration from the RR-tOE17 binding data produced a specific binding curve

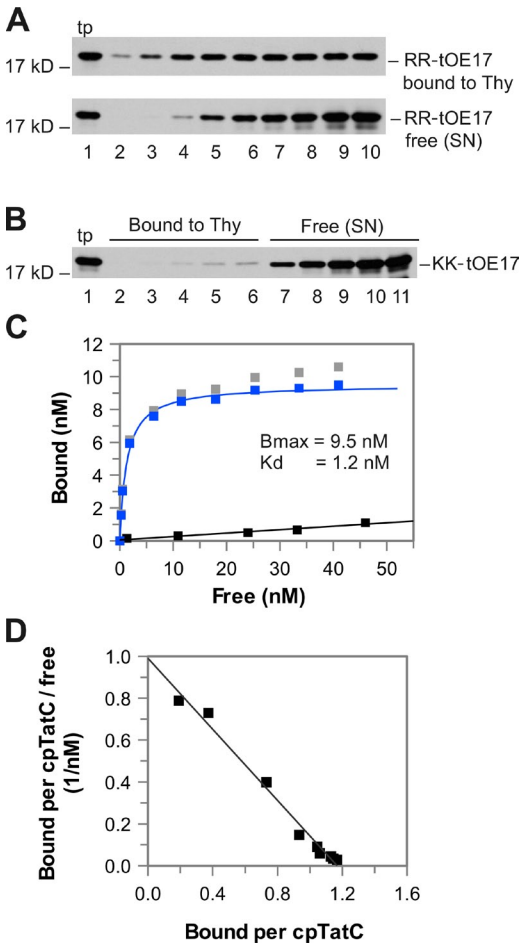

Figure 3. **Binding saturation assay with thylakoid membranes.** (A) Increasing amounts of radiolabeled RR-tOE17 were incubated with washed thylakoids (Thy) for 1 h at 4°C in a binding reaction (see Materials and methods). Recovered membranes and supernatants (SN) were used to quantify bound RR-tOE17 (top) and free RR-tOE17 (bottom), respectively. (B) Nonspecific binding was estimated in a parallel assay with KK-tOE17. tp, translation product. (C) Total bound RR-tOE17 (gray squares), nonspecifically bound KK-tOE17 (black squares and line), and specifically bound RR-tOE17 (total minus nonspecific binding; blue squares and line) were plotted versus free unbound precursor. Specific binding was fit to a single binding site model (solid blue line; see Materials and methods). The [cpTatC] in the experiment was 8.1 nM. This is a representative experiment of four repeats. (D) Scatchard analysis of specific binding data. The plotted data are from a single representative experiment out of four independent repeats.

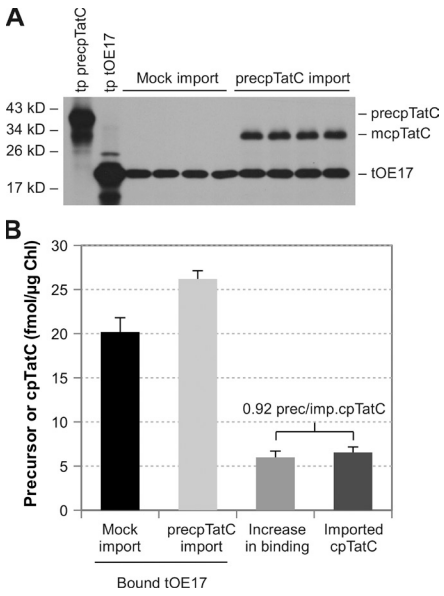

Figure 4. **Import of cpTatC into chloroplasts increases thylakoid binding capacity by approximately one precursor per imported cpTatC.** (A) Chloroplast import reactions were conducted with radiolabeled precpTatC or mock translation mixture (see Materials and methods). Recovered chloroplasts were treated with thermolysin, repurified, and used to isolate thylakoid membranes. Parallel binding assays were conducted with saturating concentrations of tOE17 (see Materials and methods). A fluorogram of samples recovered from binding assays is shown. tp, translation product. (B) Radiolabeled imported cpTatC and tOE17 were quantified by scintillation counting. The increase in binding was obtained as the difference in the amount of bound tOE17 between thylakoids with imported (imp.) cpTatC and thylakoids from the mock import reaction. Error bars represent the mean ± SD (n = 3). Chl, chlorophyll.

that asymptotically approached saturation at higher tOE17 concentrations (Fig. 3 C). Specifically bound tOE17 data were fit by nonlinear regression to a single-site binding model to obtain maximum binding (B_{max}; Fig. 3 C), which was divided by the amount of cpTatC in each assay to give a binding stoichiometry of 1.27 (SD 0.22) tOE17 per cpTatC for four biological replicates. Essentially, the same stoichiometry was obtained by Scatchard analysis of the binding data (Fig. 3 D). The dissociation constant (K_d) from four biological replicates was 1.07 nM (SD 0.09; Fig. 3 C).

Binding curves were also analyzed for any indication of cooperativity. The Hill coefficient for the four binding curves was 1.09 (SD 0.18), as determined by curve fitting to a binding isotherm equation containing a Hill parameter (see Materials and methods). Because in practice cooperativity is most evident in the middle region of the binding isotherm, a binding experiment with additional data points in this region of the curve was conducted and the data subjected to Hill analysis, which gave a Hill coefficient of 1.18 (Fig. S3). This indicates that there is no cooperativity of binding, i.e., no interaction between sites in the receptor complex.

The increase in binding sites that result from importing precpTatC into chloroplasts is approximately one per imported cpTatC

Additional approaches measured the tOE17/cpTatC binding stoichiometry at saturation. The first is based on previous observations that cpTatC imported into purified chloroplasts exhibits all of the characteristics of endogenous cpTatC (Fincher et al., 2003). IVT radiolabeled precpTatC (precursor to cpTatC) was imported into chloroplasts, and the thylakoids isolated from those chloroplasts were used for saturation-binding reactions (Fig. 4 A). The increase of tOE17 bound was determined by subtracting the amount bound by thylakoids isolated from chloroplasts from a mock import reaction. Note that in this approach, both the bound tOE17 and the imported cpTatC were determined by radiolabel counting alone and also that nonspecific binding does not affect the measurement. The ratio of increased tOE17 bound per imported cpTatC was 0.92 (SD 0.02; n = 4; Fig. 4 B).

Stoichiometry of tOE17 per cpTatC with purified precursor protein-bound cpTat receptor complexes

A second alternative approach involved saturating thylakoid membranes with tOE17, solubilizing the membranes with digitonin, and then purifying the receptor complexes by affinity chromatography. Two different but complementary affinity purification procedures were used, one based on affinity to a receptor component and the other based on affinity to the precursor protein. In Fig. 5 (A and C), the solubilized complexes were purified by immunoaffinity to anti-Hcf106 IgG immobilized beads (see Materials and methods). Only small amounts of tOE17 and cpTatC were present in the flow-through and wash fractions, and the total recovery of tOE17 was 85% (Fig. 5, A and C). The stoichiometry of tOE17 to cpTatC in the eluate was 0.79 (SD 0.18; $n = 3$). In the second affinity method, membranes were saturated with a C-terminally His-tagged tOE17 (tOE17-GS3-His), and solubilized complexes were purified by metal ion affinity chromatography (see Materials and methods; Fig. 5, B and D). Only small amounts of cpTatC and trace amounts tOE17-GS3-His were detected in the flow-through and wash fractions. The overall recovery of tOE17-GS3-His was 88%, and the ratio of tOE17-GS3-His to cpTatC in the eluate was 1.05 (SD 0.22; $n = 3$). The mean for the two affinity methods is 0.92 tOE17/cpTatC.

To summarize, the ratio of tOE17 per cpTatC obtained by the three different approaches—binding saturation curves, increase in binding after cpTatC import, and purification of fully occupied complexes by affinity chromatography—was 1.27, 0.92, and 0.92, respectively. The mean of the three methods, 1.04, indicates a stoichiometry of one tOE17 per cpTatC at saturation and implies that the receptor complex can bind up to eight precursor proteins (see Discussion).

All binding sites are functional for transport

Transport of receptor bound precursor protein (chase) can be modeled as a two-step reaction. In the first step, Tha4 assembles with the precursor-bound receptor. In the second step, the precursor is transported and the signal peptide cleaved by the lumenal signal peptidase to produce the mature protein. Mori and Cline (2002) used chemical cross-linking during a chase reaction to show that Tha4 assembly correlates with an initial lag phase and is temporally distinct from the transport phase. Furthermore, Tha4, which dissociated after completion of transport, reassembled when more precursor protein was added to the reaction (Mori and Cline, 2002). A simple equation for this process is $P:R+nT4 \xrightarrow{k_a} P:R:T4n \xrightarrow{k_t} R+nT4+M$, where P denotes precursor protein, R denotes receptor, T4 denotes Tha4, M denotes the transported mature protein, k_a denotes the assembly rate constant, and k_t denotes the translocation rate constant. To examine characteristics of transport in more detail, chase kinetics were analyzed with different sets of starting conditions that included tOE17 occupying ~20% versus 100% of binding sites and a range of Tha4 concentrations from 6 Tha4 per tOE17 to 115 Tha4 per tOE17 (Fig. 6). The latter was obtained by supplementing reactions with IVT

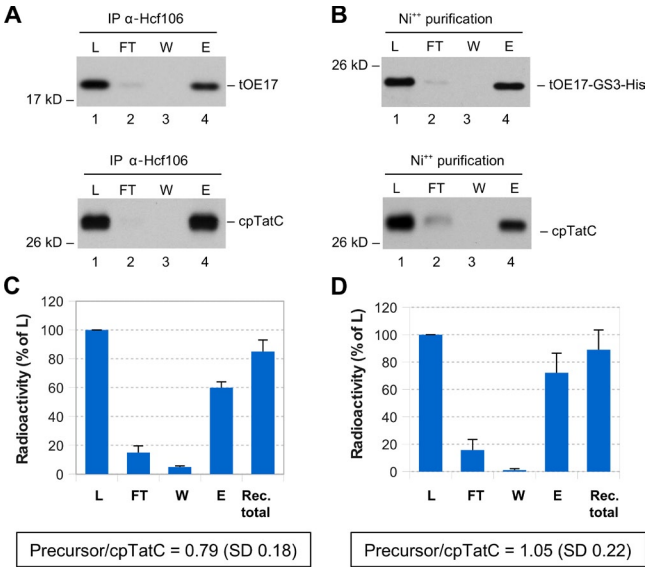

Figure 5. **Affinity-purified precursor-bound receptor complex contains approximately one precursor protein per cpTatC.** (A–D) Thylakoids were incubated with saturating amounts of tOE17 (A and C) or tOE17-GS3-His (B and D) in a binding reaction. Recovered thylakoids were solubilized with digitonin, and the insoluble pellet was removed by centrifugation. (A and C) The soluble extract (load; lane L) was incubated with α-Hcf106 IgG beads, and the unbound material (lane FT) was removed after centrifugation. The recovered beads were washed (lane W) and then eluted with SDS buffer containing urea (lane E). (A) The tOE17 in the load and all fractions was detected by fluorography and cpTatC by immunoblotting. IP, immunoprecipitation. (C) The tOE17 in each fraction is shown as a percentage of starting material. Error bars represent the mean ± SD ($n = 3$). (B and D) The soluble digitonin extract from a binding reaction with tOE17-GS3-His (lane L) was incubated with Ni–nitrilotriacetic acid magnetic beads, and the unbound fraction (lane FT) was removed after magnetic separation. The beads were washed (lane W) and then eluted (lane E), and the fractions were subjected to fluorography and immunoblotting (B). The tOE17 in each fraction is displayed as the percentage of starting material. Error bars represent the mean ± SD ($n = 3$; D). The tOE17 and cpTatC were quantified in the elution (see Materials and methods). Total recovery (Rec. total) of tOE17 represents the amount of precursor present in the FT, W, and E fractions.

Tha4 (Dabney-Smith et al., 2003). Transport was scored by the appearance of the mature form of OE17 (mOE17; see Materials and methods). As shown in Fig. 6, in three out of four of the conditions (including one in which all sites were occupied with precursor protein), ~90% of the initially bound tOE17 was transported in 25–30 min, which is consistent with ≥90% specific and ≤10% nonspecific binding (Fig. 2). This indicates that all binding sites are functional for transporting their bound precursor protein.

Transport kinetics of these three cases (Fig. 6, A–C) consisted of a lag phase followed by a rapid translocation phase. Our attempts to solve for both k_a and k_t for chase reactions were not feasible. This is probably because, in nearly all situations, the Tha4 concentration significantly changes during the assembly step in an undefined manner (see Materials and methods). However, for situations in which [Tha4] is sufficient to functionally assemble all of the bound precursor sites (i.e., [P] = [P:R:T4n]), the rate of translocation equal to $k_t \times$ [P] and k_t can be determined by a fit of either [tOE17] or [mOE17] versus time during the translocation step (see Materials and methods).

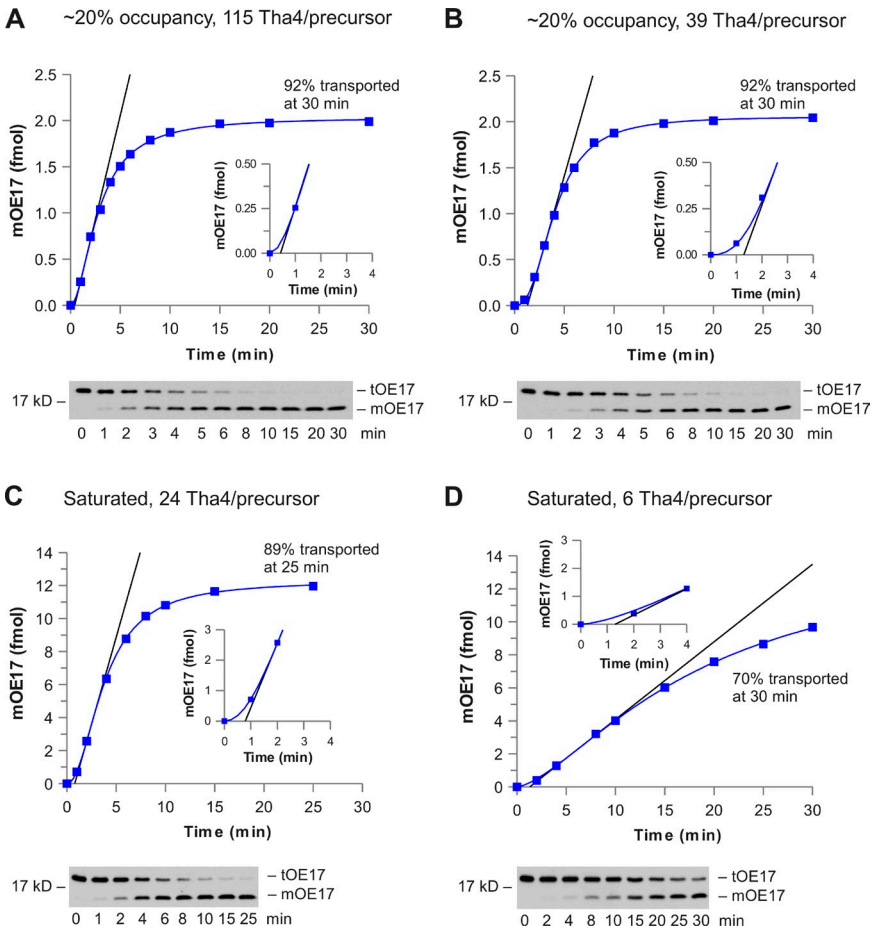

Figure 6. **Kinetics of bound tOE17 transport in 20% precursor-saturated and 100% saturated membranes with sufficient and insufficient Tha4.** (A–D) Thylakoid membranes were incubated in binding reactions with concentrations of tOE17 that resulted in 20% (A and B) or 100% (C and D) saturation of receptor complexes. After binding, thylakoids were incubated with IVT Tha4 (A and C) or with mock translation mixture (B and D). Transport of bound tOE17 (chase) was started with ATP and transfer to a 15°C light bath followed by sampling at time points (see Materials and methods). The transported OE17 (mOE17) was fit to a sigmoidal equation (blue lines). Tangent lines (black) were drawn at the inflection point of each curve and used to determine the lag times (see Materials and methods). Fluorograms of chase reactions are displayed below the panels. In the plots, note the differences in y-axis scales between 20% saturated and 100% saturated membranes. The data are from a single representative experiment out of three independent repeats.

The translocation step was separately analyzed by subtracting the lag time (Fig. 6) from chase datasets (see Materials and methods). For three of the chase reactions shown in Fig. 6, in which the Tha4/tOE17 was 24, 39, and 115, the data fit an exponential first-order kinetic model (Fig. 7). When the data were plotted as the percentage of mOE17 produced by the end of each reaction (i.e., to normalize differences in the initial [tOE17]), the three curves could be virtually superimposed (Fig. 7) and yielded very similar k_t values of ~0.3 min^{-1}. This suggests that ~25 Tha4/tOE17 are sufficient to functionally assemble a transport site. In support of this, the k_t values for the translocation phase in experiments in which Tha4 per tOE17 was ≥25 were 0.27 min^{-1} (SD 0.04; $n = 5$) for tOE17-saturated receptors and 0.31 min^{-1} (SD 0.05; $n = 5$) for low-occupancy receptor complexes. *T* test analysis indicates that these values are not statistically different. The nature of first-order kinetics, in this case rate = $k_t \times$ [tOE17], is that all precursor protein-bound sites have an equivalent probability of transporting their bound precursor (Fig. 7). This does not mean that all sites transport simultaneously but that all sites are independently active for transport. Although the k value of ~0.3 min^{-1} (approximate transport time, τ, of 3 min) is rather slow for a protein translocation reaction, these assays were conducted at 15°C (to facilitate sampling); increasing the temperature of the chase reaction to 25°C increased the k_t value at least twofold, resulting in τ = ~1.5 min (unpublished data).

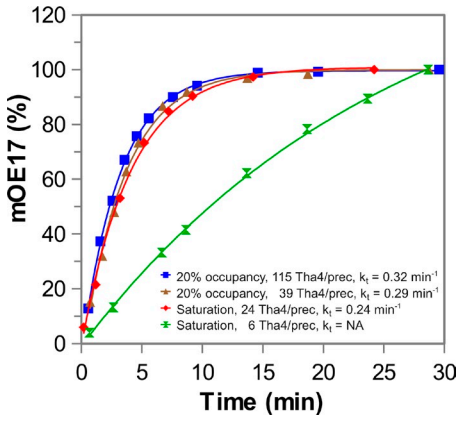

Figure 7. **Analysis of the translocation phase in lag-subtracted chase reactions.** The lag time from each chase experiment shown in Fig. 6 was subtracted from datasets, and the resulting data were plotted as the percentage of the final amount of mOE17 and fit to an exponential first-order equation (see Materials and methods). The k_t values for the translocation phase in experiments in which Tha4 per tOE17 was ≥25 were 0.27 min^{-1} (SD 0.04; $n = 5$) for tOE17-saturated receptors and 0.31 min^{-1} (SD 0.05; $n = 5$) for low-occupancy receptor complexes. The plots of data shown are from a single representative experiment out of three independent repeats.

In the fourth chase reaction, the receptor complexes were saturated with precursor protein, but the Tha4/tOE17 was only six (Fig. 6 D). Translocation occurred at a much slower rate and was essentially linear for 15 min before slowly

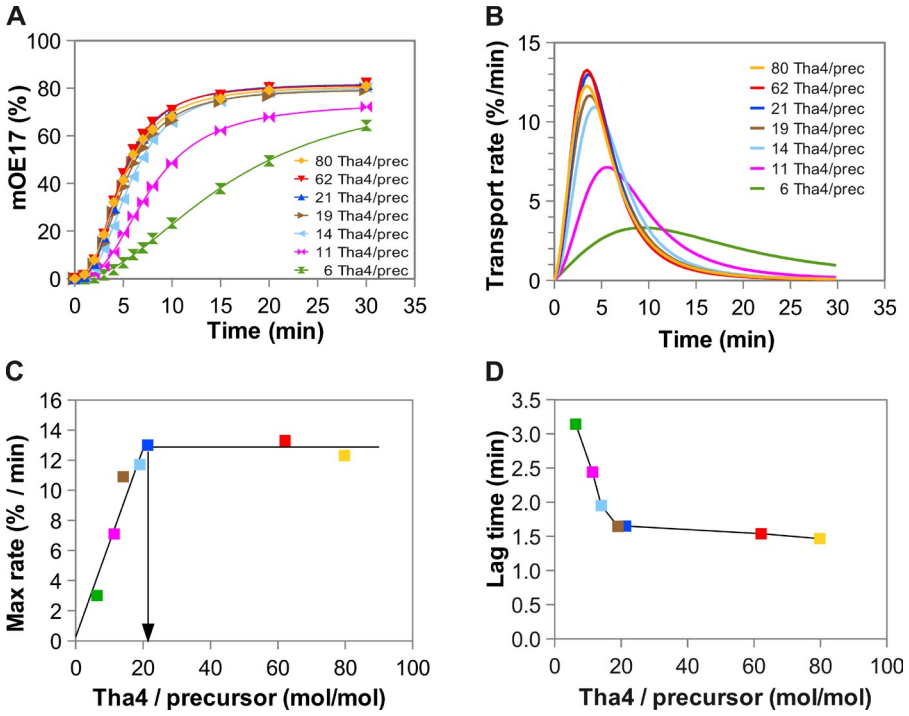

Figure 8. **The Tha4 oligomer required to transport an OE17 precursor contains ~26 Tha4 protomers.** Chase reactions with tOE17-saturated membranes were conducted with different amounts of IVT Tha4 (see Materials and methods). (A) Transport of tOE17 was quantified as the amount of mOE17 produced and plotted as the percentage of tOE17 at time 0, and the data were fit to a sigmoidal equation (see Materials and methods). (B) Instantaneous transport rates for each chase reaction were estimated with the first derivative of the fitted curves. (C) The amount of Tha4 (quantitative immunoblotting) per precursor protein (radiolabel) was estimated for each chase reaction (see Materials and methods) and plotted versus the highest instantaneous transport rates (Max rate). Regression lines for the chase reactions with <25 Tha4/tOE17 and for the chase reactions with 21–80 Tha4/tOE17 are shown. The intercept of the two lines (arrow) represents the Tha4 sufficiency point (21 Tha4 per precursor) for transport of tOE17. The mean sufficiency point for the three independent measurements was 26 (SD 6.3). (D) Lag times were estimated, as in Fig. 6, and plotted versus Tha4/tOE17. Data points in C and D are colored and correspond to the chase reactions shown in A and B. The plots of data in the figure are from a single representative experiment out of three independent repeats.

falling off (Fig. 7). This would be consistent with a situation in which the available Tha4 functionally assembled only a fraction of the tOE17-bound sites initially and, after transport of those precursor proteins, recycled to new tOE17-bound sites (Fig. 7).

The minimal Tha4 oligomer required to transport an OE17 precursor has ~26 protomers

If this interpretation is correct, it should be possible to more precisely titrate the Tha4/tOE17 ratio to find the minimal Tha4/tOE17 to functionally assemble all of the tOE17-bound sites. This was accomplished with a series of chase reactions with tOE17-saturated membranes in which the Tha4/tOE17 was varied from 6 to 80 with IVT Tha4 (Fig. 8). The highest instantaneous rate of transport for each chase reaction was determined from the first derivative of a sigmoidal fit of the dataset, as described in Materials and methods (Fig. 8, A and B). The highest instantaneous rates occurred immediately after the lag, when available Tha4 is maximally assembled with tOE17-occupied sites (e.g., see Fig. 8 B). As shown in Fig. 8 C, the highest instantaneous transport rates for the different chase reactions increased linearly with Tha4/tOE17 ratios from 6 to ~20 (Fig. 8 C). Increases in the Tha4/tOE17 above ~20 did not further increase the rate. The intersection of the lines can be considered to be the point of Tha4 sufficiency (Fig. 8 C). The linear increase in the highest instantaneous rate with Tha4/tOE17 followed by an abrupt leveling at the maximum obtainable rate supports the interpretation that below the sufficiency point, Tha4 functionally assembles a fraction of the available sites and that at the sufficiency point and above, Tha4 functionally assembles all tOE17-occupied sites. The mean sufficiency point from three independent experiments, 26.4 Tha4/tOE17 (SD 6.3), represents the size of the Tha4 oligomer required to transport one tOE17.

A slightly different experimental design was used as an alternative approach to determining the sufficiency point. Rather than varying [Tha4] to achieve a range of Tha4/tOE17 ratios (Fig. 8), endogenous Tha4 was the only source of Tha4 (i.e., constant [Tha4]), and the amount of bound tOE17 was varied (Fig. 9). A similar biphasic curve (as that in Fig. 8) was obtained for a plot of the highest instantaneous transport rate (expressed as the percentage of initial [tOE17] per minute) versus Tha4/tOE17 (Fig. 9 B). This is important because it confirms that the highest transport rates vary with the Tha4/tOE17 ratio rather than Tha4 concentration per se. It also supports the conclusion that the plateau in transport rate above the breakpoint is a result of Tha4 sufficiency rather than, e.g., the result of some conceivable limitation to incorporating high concentrations of Tha4 into thylakoids.

The mean sufficiency point obtained from two independent experiments with this later approach was ~45 Tha4/tOE17. This might mean that IVT Tha4 is more active than endogenous Tha4. However, we think that this ratio is an overestimate as a result of a pool of unavailable Tha4 in reaction mixtures of Fig. 9. Previous work showed that Tha4 is associated with the plastid envelope in ruptured chloroplast preparations (Fincher et al., 2003). Envelope membrane vesicles are present in the stromal extract added to chase reactions and are also a persistent contaminant of isolated thylakoids (Douce and Joyard, 1982; Dorne et al., 1990). Envelope-associated Tha4 in our assays is estimated to be up to ~30% of the total (Table 1). When corrected for the ~30% presumably unavailable Tha4, the mean Tha4 sufficiency point was 31 Tha4/tOE17 (e.g., see Fig. 9 C),

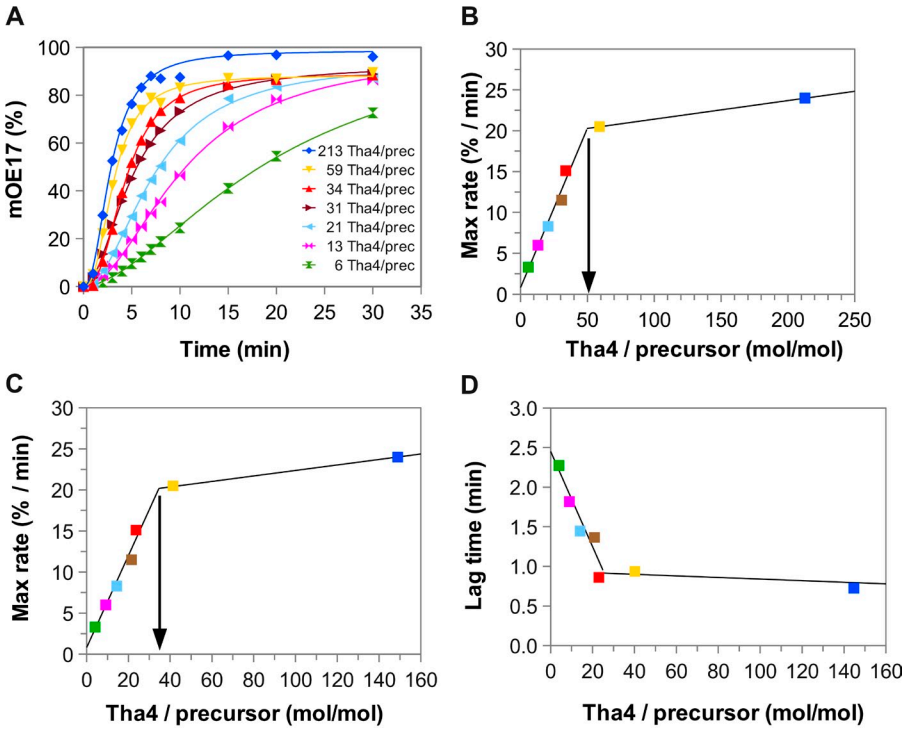

Figure 9. **Estimation of the minimal Tha4 oligomer size for optimal transport relying only on endogenous Tha4.** Binding reactions were conducted with varying concentrations of tOE17. Chase reactions were conducted without added Tha4 (see Materials and methods). (A) The amount of transported OE17 (mOE17) was plotted as the percentage of the total amount of tOE17 at time 0 and fit to a sigmoidal equation. (B) Tha4 per tOE17 for each chase reaction (see Materials and methods) was plotted versus the highest instantaneous transport rates (Max rate), as estimated from the first derivative of the fitted sigmoidal curves. (C) Tha4 concentrations were corrected by an estimate of nonavailable Tha4 and plotted versus the highest instantaneous transport rates. A regression line was drawn for chase reactions with increasing highest instantaneous rates, and a straight line was drawn for the two chase reactions that had achieved the maximum rate. (B and C) The intercept between the two lines indicates the Tha4 sufficiency point (arrows). (D) The lag time for each chase reaction was plotted versus the corrected Tha4/tOE17 ratio. The data points in B, C, and D are colored and correspond to the chase reactions shown in A. The data are from a single representative experiment out of two independent repeats. The corrected Tha4/tOE17 sufficiency point for the two experiments was 31.

which is within the variance of the 26.4 (SD 6.3) obtained in the chase reactions supplemented with IVT Tha4 (Fig. 8).

The lag phase is dependent in part on the relative Tha4 concentration

As described in the previous section, the Tha4 assembly phase of the reaction is thought to involve Tha4 diffusion to and assembly with precursor-bound sites. A consistent relationship was found for lag time versus Tha4/tOE17 (Figs. 8 D and 9 D). In both experimental approaches, lag time decreased with increasing Tha4/tOE17 and then leveled off (Figs. 8 D and 9 D). Interestingly, the leveling off of lag occurred near the Tha4/tOE17 sufficiency breakpoint. The two phases of lag suggest that assembly involves more than Tha4 diffusion to the receptor, possibly also involving a rearrangement or redistribution of Tha4 before the translocase becomes transport active.

Discussion

This study addressed the stoichiometry of precursor protein binding to the cpTat receptor complex and the stoichiometry of Tha4 required for transport. Three different methods were used to determine the binding stoichiometry of precursor protein per cpTatC. These methods, using both intact membranes and purified membrane complexes, gave remarkably similar ratios of approximately one bound tOE17 per cpTatC, providing strong support for a 1:1 stoichiometry. This suggests that each receptor complex can concurrently bind approximately eight precursor proteins, based on an estimate of the number of cpTatC per receptor complex. The isolated thylakoid receptor complex contains only cpTatC and Hcf106 (unpublished data), similar to the *E. coli* TatBC complex (McDevitt et al., 2006; Orriss et al., 2007), and migrates on blue native PAGE at ∼700 kD. After correcting for the contribution of bound Coomassie blue to the apparent molecular mass (Heuberger et al., 2002), the estimated number of cpTatC-Hcf106 heterodimers is ∼7.5 per complex, which compares well with structural results for the *E. coli* TatBC receptor complex (Tarry et al., 2009). Analysis of the transport step suggests that all precursor protein-bound receptor sites can be individually activated for transport and, furthermore, suggested a minimal Tha4 oligomer size of ∼26 protomers for transporting an OE17 precursor protein. This implies that, for tOE17, a functional Tat translocase unit consists of one cpTatC (one Hcf106) and ∼26 Tha4.

The binding stoichiometry obtained here is higher than that reported by Tarry et al. (2009), who found one to two precursor proteins per purified *E. coli* TatBC receptor complex. The discrepancy may be a result of dissociation of precursor proteins from the TatBC complex during purification procedures. The tOE17–cpTatC:Hcf106 complex was stable to the purification procedures used here (Fig. 5). However, we have previously observed precursor dissociation from the thylakoid receptor complex during electrophoresis on blue native polyacrylamide gels, the extent of which varied with the nature of the bound precursor (Cline and Mori, 2001; Gérard and Cline, 2007; Ma and Cline, 2010). Clearly, the stoichiometry obtained for purified receptor complexes will depend on the harshness of the purification method and the dissociation constants of each particular precursor protein. Binding of tOE17 exhibited a K_d of ∼1 nM and very slow dissociation at 0–15°C, whereas the precursors used by Tarry et al. (2009) have apparent K_d values of 50–100 nM, although recent estimates from a fluorescence resonance energy transfer–based assay suggest a K_d for preSufI of 7–23 nM (Whitaker et al., 2012). This may explain, in part,

the low number of preSufI and CueO precursors that Tarry et al. (2009) recovered with purified complexes.

The high affinity of tOE17 for the cpTat receptor minimized nonspecific binding to the membrane bilayer (Fig. 2), which increases linearly with precursor protein concentration (Fig. 3). Other binding studies with *E. coli* inverted vesicles (Bageshwar et al., 2009) and thylakoid membranes (Musser and Theg, 2000; Hou et al., 2006) have observed precursor protein binding to the lipid bilayer and have further suggested that binding to the bilayer is an intermediate in the binding pathway. Although we can't exclude this possibility, our results here (Fig. 6) and in unpublished studies indicate that lipid-bound tOE17 present at the start of a chase reaction was not productive, i.e., it was not transported during the chase reaction. Nevertheless, lipid-bound precursor proteins did not impact the results and conclusions of the present study because it was a very low percentage of total binding and was effectively subtracted (Fig. 3) or eliminated (Figs. 4 and 5) from the analyses.

Multivalent receptors frequently exhibit cooperativity, wherein binding to one site alters the affinity of other sites in the complex. The issue of cooperativity for the Tat transport system has been a matter of debate. Tarry et al. (2009) argued for a negative binding cooperativity for the *E. coli* Tat system to explain, in part, the fact that TatBC complexes contained only one or two bound precursor proteins. Alder and Theg (2003) reported positive cooperativity for translocation of the OE17 precursor protein, although it was not determined whether this occurred at the binding step or the translocation step. On the other hand, a similar study of translocation of the OE23 precursor found no evidence for cooperativity (Cline et al., 1993). The present study specifically examined the binding step and found no evidence of cooperativity, as judged by a Hill coefficient of $\sim$1 (Figs. 3 and S3). Although it is conceivable that the enhanced affinity of the tOE17 precursor obscured cooperative interactions, we think this is unlikely because of the quality of the data in the lower to middle regions of the binding curves (Figs. 3 and S3).

Analysis of the translocation of bound tOE17 (chase) gave considerable insight into the mode of cpTat transport and the involvement of Tha4. When Tha4 was present in excess, the translocation step was described by a first-order kinetic model in which the instantaneous rate of transport equals $k_t \times$ [bound precursor]. More importantly, with Tha4 excess, the k_t values determined for a wide range of receptor complex occupancies, from well below one precursor per complex (Fig. 9) to fully saturated complexes (Figs. 7 and 8), were statistically identical. This observation is most easily interpreted to mean that all precursor-bound sites are independently competent for transport and can be concurrently active for transport. That is not to say that all precursor proteins bound to a receptor complex are simultaneously transported, although simultaneous transport can apparently occur in certain cases (Ma and Cline, 2010). Rather, it says that all sites have the same probability of undergoing translocation. If, for example, only one binding site was active per complex at a time, there would be a sequential progression of transport around a complex, and transport should be linear with time for extended periods rather than exponential.

The relationship between the relative amount of Tha4 and translocation rate was especially informative. The observation that above a threshold Tha4/tOE17 value the transport rate was maximum and constant (Figs. 8 and 9) strongly suggests that the threshold value is the point at which Tha4 has functionally assembled all tOE17-bound sites for transport. Its value of $\sim$26 Tha4/tOE17 can be interpreted to mean that a 26-Tha4 oligomer complex facilitates transport of one tOE17 precursor protein. Two previous studies reported a measure of Tha4 (TatA) oligomer size in a functional context. An in vitro disulfide cross-linking study produced oligomers up to 18 Tha4 via C-tail Cys residues when Tha4 was assembled with the translocase in transporting membranes (Dabney-Smith and Cline, 2009). Fluorescence imaging of *E. coli* TatA-YFP (Leake et al., 2008) observed spots of variable size in the Tat-transporting *E. coli* cells with a median spot size of 25 TatA-YFP. Limitations of the techniques in these studies (i.e., inefficiency of disulfide cross-linking and uncertainty regarding the number of precursor-bound sties per TatA-YFP spot) precluded an estimate of the transport-active oligomer size. However, it is interesting that the Tha4 (TatA) oligomer sizes obtained are similar to our functional estimate (e.g., Fig. 8) as well as the stoichiometry of Tha4 per cpTatC in chloroplasts (Table 1).

Our results showing that precursor protein binding is non-cooperative and that all sites can be independently transport active raise the question of what advantage Tat might gain by organizing receptor units into a multivalent complex. One possibility is that when Tha4 is limiting, Tha4 oligomers could move to adjacent sites on the receptor complex without dissociation and reassembly. This would explain the observation that at very low Tha4/precursor ratios, the transport rate was nearly constant (Figs. 7 and 9), consistent with an absence of extensive lag for Tha4 recycling. Such a mechanism would provide an efficiency advantage for the steady-state operation of the cpTat system during periods of rapid thylakoid biogenesis.

Oligomeric Tha4 (TatA) is considered to serve as the protein-conducting component of the Tat system, and emerging data indicate that TatA contacts the mature domain of the precursor (Panahandeh et al., 2008; Maurer et al., 2010; Fröbel et al., 2011). The functional Tha4 oligomer size is tantalizing to view in the context of models for Tat transport. One model is that Tha4 (TatA) assembles appropriately sized oligomeric channels through which the bound precursor protein crosses to the trans side of the membrane (Gohlke et al., 2005; Leake et al., 2008). Another is that Tha4 (TatA) oligomers destabilize the bilayer structure and facilitate bound precursor protein movement across the membrane (Brüser and Sanders, 2003), possibly similar to the way that amphipathic antimicrobial peptides function (Tossi et al., 2000). If proteins are transported through structural channels, the size of the oligomer should be tightly linked to the molecular dimensions of the protein substrate but relatively unaffected by other assay parameters. Gohlke et al. (2005) estimated that 19 TatA protomers would provide a 30–35-Å channel, sufficient for the OE17 precursor. If the substrate protein is transported through the Tha4-destabilized membrane bilayer, the oligomer size may not be as dependent on substrate dimensions but instead sensitive to

temperature and other factors that influence the fluidity and stability of the membrane, such as the presence of nonbilayer-forming lipids or the degree of saturation of the polar lipids. Of interest, a study of thylakoid transport characteristics in fatty acid desaturase mutants of *Arabidopsis* found that in membranes with increased fatty acid saturation (decreased fluidity), the activity of the cpTat system was decreased, whereas the activity of the cpSecA-SecYE system was increased (Ma and Browse, 2006).

Future studies to determine the relationship between the functional size of the Tha4 oligomer, precursor protein dimensions, composition of the membranes, and other parameters of the assay should provide considerable insight into the mechanism of protein translocation by the Tat system. At present, the translocation step is the most poorly understood aspect of Tat transport.

Materials and methods

Source plants, chloroplasts, and thylakoid isolation
Intact chloroplasts were isolated from 9–10-d-old pea seedlings (Progress #9 Improved; Buckeye Seed & Supply) and were resuspended in import buffer (IB; 330 mM sorbitol and 50 mM Hepes-KOH, pH 8.0; Cline et al., 1993). Isolated thylakoids were obtained from intact chloroplast by osmotic lysis followed by centrifugation and were washed and resuspended in IB containing 5 mM $MgCl_2$ (IBM). Chlorophyll concentrations were determined according to Arnon (1949). There are 10^6 pea chloroplasts or thylakoids per microgram of chlorophyll (Chen et al., 1990; Cline et al., 1993), and the thylakoid network remains intact after chloroplast lysis.

Plasmid construction and mutagenesis
Transcription clones for tOE17 V-20F (Gérard and Cline, 2007), precpTatC and mcpTatC (mature cpTatC; Mori et al., 2001), and mTha4 (Fincher et al., 2003) are as previously described. The DNA clones for the His-tagged tOE17 precursor and His-tagged cpTat components (cpTatC, Hcf106, and Tha4) were constructed by PCR mutagenesis using the QuikChange kit (Agilent Technologies) by adding an unstructured linker consisting of three GGGGS repeats and six histidine residues at the C terminus of the protein. The DNA clone for KK-tOE17 precursor was constructed by PCR mutagenesis of RR-tOE17 using the QuikChange kit. DNA sequencing on both strands at the University of Florida Interdisciplinary Center for Biotechnology Research DNA Sequencing Core Facility verified cloned constructs.

Preparation of radiolabeled precursor proteins
Capped RNAs were transcribed with SP6 polymerase (Promega) and translated in the presence of [^{3}H]-Leu with a homemade wheat germ (WG) translation system (Cline, 1986). Translation reactions were incubated for 1 h at 25°C and stopped with 1 vol of 2× IBM containing 400 µM cycloheximide.

Quantification of IVT radiolabeled proteins
The specific radioactivity for [^{3}H]-Leu in translation reactions was determined for each WG translation preparation by isotope dilution experiments. A series of translation reactions were performed with a fixed amount of [^{3}H]-Leu and increasing amounts of unlabeled Leu in a range from 0–80 µM final concentration (Fig. S1). Radiolabeled translation products were extracted from SDS-PAGE/fluorography gel slices (Cline, 1986), and dpm were measured by scintillation counting in a scintillation counter (LS6500; Beckman Coulter) calibrated for tritium and chemical and color quench. The reciprocal of the radioactivity was plotted against the total known Leu concentration in the reaction (added unlabeled Leu + [^{3}H]-Leu), yielding the concentration of unlabeled Leu in the WG extract as the negative y-axis intercept (Fig. S1; Patrick et al., 1989). The nanomoles of translated protein were determined using the specific radioactivity of Leu in the translation reaction, the dpm of the gel-extracted protein, a correction for the number of Leu residues per protein, and a correction for the extraction efficiencies determined for each protein (Table S1).

Quantitative immunoblotting
Samples received 1 vol of sample buffer (4% SDS, 66% glycerol, 5% β-mercaptoethanol, 2 mM EDTA, and 125 mM Tris, pH 6.8) and were incubated at 37°C for 20 min. Samples were analyzed on gels containing the minimum percentage of acrylamide to maximize electrotransfer (9% acrylamide gels for cpTatC and Hcf106 and 12.5% for Tha4). Samples were loaded in gel lanes with a syringe. Gels were electroblotted to 0.2-µm pore-sized polyvinylidene fluoride membranes (cpTatC) or 0.2-µm pore-sized nitrocellulose membranes (Hcf106 and Tha4) for 60 min in a wet tank system with 200 mM glycine, 25 mM Tris, and 20% methanol. Blots were incubated with primary antibodies for cpTatC, Hcf106, and Tha4 (Mori et al., 1999; Mori et al., 2001) and developed with the ECL method (GE Healthcare) according to the manufacturer's instructions. Immunoblot films were scanned at 600 dots per inch in translucent mode with a scanner (Perfection 3170; Epson) followed by image analysis by densitometry with Quantity One software (Bio-Rad Laboratories; Fig. S1 C). The amounts of the particular proteins were determined by comparison with full-length IVT protein standards (Fig. S1 C) and corrected for aggregation on gels (Table S1) and for inefficient electrotransfer of membrane-associated proteins (Table S2).

Chloroplast import and thylakoid protein integration assays
Radiolabeled precpTatC was incubated with isolated chloroplasts (0.33 mg chlorophyll/ml) and 5 mM Mg-ATP in IB with 120 µE/m^2/s of light in a 25°C water bath for 30 min. After import, chloroplasts were treated with thermolysin and then repurified by centrifugation through a Percoll cushion (Cline et al., 1993). Recovered chloroplasts were lysed hypotonically, and, thylakoids recovered by centrifugation were washed once and resuspended to 1 mg chlorophyll/ml. Integration of IVT Hcf106 and Tha4 into isolated thylakoids was performed by incubating translation mixtures with washed thylakoids (0.5 mg chlorophyll/ml) at 25°C in the dark for 20 min. After integration, membranes were washed twice and resuspended in IBM.

Precursor protein-binding assay
IVT precursor proteins were treated with apyrase (10 U per 100-µl translation) for 30 min on ice to remove nucleoside triphosphates. Binding reactions were performed by incubating precursor proteins with isolated thylakoids in the dark at 4°C with end-over-end mixing for 1 h. Binding reactions with different amounts of precursor protein were prepared by diluting IVT precursor with apyrase-treated mock translation reaction mixture. Thus, all binding reactions contained an equal concentration of translation components. Typically, binding reactions contained 40 µg chlorophyll of thylakoids and 120 µl of precursor protein in low-retention microfuge tubes. After binding, the unbound supernatant and bound thylakoid fractions were recovered by centrifugation, and the thylakoids were washed twice, changing tubes each time. Resuspended thylakoids were mixed with 1 vol 2× SDS buffer without tracking dye and chlorophyll concentrations measured to adjust samples for equal loading.

Binding saturation data analysis
Specific binding curves were obtained by subtracting nonspecific binding, determined with KK-tOE17 in parallel assays, from total binding of RR-tOE17. Specific binding data were fit by nonlinear regression to a single-site binding equation, $B = B_{max} \times [precursor]/(K_d + [precursor])$, where B denotes the concentration of bound precursor, [precursor] denotes the concentration of free precursor, and the fitting parameters B_{max} and K_d denote the maximum binding and the dissociation constant, respectively, using LabPlot-GNU software. The Hill coefficient in binding saturation assays was determined in two different ways. Specific binding data were fit to a single-site binding equation including a Hill slope term (h), $B = B_{max} \times [precursor]^h/(K_d^h + [precursor]^h)$, where h is the Hill coefficient. Alternatively, the Hill slope was determined by plotting the $\log(\theta/(1-\theta))$ versus Log [precursor], where θ is the fraction of occupied sites (specific binding/B_{max}) and [precursor] is the concentration of free unbound precursor protein in each binding reaction. The Hill coefficient is the slope of the regression line of the plotted data.

Precursor protein chase assay
For transport assays of bound precursor protein (chase), thylakoids recovered from binding assays equivalent to 25 µg of chlorophyll were further incubated on ice for 20 min in the dark with 75 µl containing varying amounts of apyrase-treated IVT unlabeled mTha4. mTha4 dilutions were made with apyrase-treated mock translation extract. Reaction mixtures then received 75 µl of stromal extract and were transferred to a 15°C water bath for 5 min in the dark. Aliquots were removed as time 0 samples, and

chase reactions were initiated with Mg-ATP (12 mM final concentration) and ~100 μE/m^2/s white light at 15°C. At time points, 10-μl aliquots were removed, mixed with SDS buffer, and heated at 95°C for 3 min. Samples were analyzed by SDS-PAGE and fluorography, and transport was quantified by scintillation counting of the tOE17 and mOE17 bands. Two observations indicate that appearance of mOE17 accurately measures transport. Hashimoto et al. (1997) showed that the OE17 precursor is not processed until the entire protein is across the membrane. Second, time-course analysis in which reactions were terminated rapidly with $HgCl_2$ (Reed et al., 1990) showed that all transported proteins had been processed to mature form (unpublished data). Chase reactions were conducted at 15°C rather than 25°C to slow the reaction, permitting sampling of more time points in the rapid phase of translocation.

Chase kinetics data analysis

The amount of mOE17 obtained for each time point was corrected for recovery and fit by nonlinear regression to a sigmoidal equation. Several sigmoidal models were attempted, including Boltzmann Sigmoidal, Sigmoidal dose response with variable slope (Prism 5; GraphPad Software), and a two-consecutive irreversible first-order reaction model (Connors, 1990). However, the two-step irreversible model only converged when [Tha4] was pseudoconstant, i.e., either a very high amount of Tha4 or a very low and recycling amount of Tha4. We found that all of the data points, especially in the lag phase, were best fit to a generic sigmoidal equation, $y = a \times x^b/(c^b + x^b)$, where y equals mOE17, x equals time, and a, b, and c are fitting parameters. The highest instantaneous transport rate in each chase reaction was obtained from the first derivative of the fitted sigmoidal curve by numerical differentiation using LabPlot-GNU. The lag time for each reaction was estimated by the x-axis intercept of the tangent line to sigmoidal curve at the point of highest instantaneous transport rate (Auer and Kashchiev, 2010). Lag times were subtracted from chase datasets, which were plotted and fitted to a first-order exponential equation, $y = a \times e^{(-k \times t)} + c$, where y equals [mOE17], a denotes [tOE17] present at time 0, k is the rate constant, and t is time. Similar methodology is described in Weimer et al. (1990) and Gettens and Gilbert (2007).

Solubilization and purification of precursor-bound receptor complexes

Thylakoids recovered from binding assays with saturating concentrations of precursor protein or His-tagged precursor protein were solubilized with digitonin, 0.5× IB, 20% glycerol, 0.5 M aminocaproic acid, and 2 mM PMSF, as previously described (Gérard and Cline, 2007). Insoluble material was removed by centrifugation at 150,000 *g* at 2°C for 30 min, and the supernatant was removed for subsequent affinity purification. For nondenaturing immunoprecipitation, the supernatant was incubated with Hcf106-IgG cross-linked to protein A Sepharose beads and mixed end over end for 2 h at 4°C (Cline and Mori, 2001). Unbound proteins were recovered by centrifugation, and the beads were washed with 0.5% digitonin, 0.5× IB, 0.5 M aminocaproic acid, and 20% glycerol for 10 min at 4°C. Bound proteins were recovered by incubating the beads with 2× SDS, 8 M urea, and nonreducing SDS buffer for 16 h at room temperature and removing the beads with a mini spin column (Promega).

For affinity purification to Ni–nitrilotriacetic acid magnetic agarose beads (QIAGEN), the 150,000-*g* supernatant was combined with beads and 1 vol of 40 mM Hepes, pH 7.8, 300 mM NaCl, and 40 mM imidazole and mixed end over end at 4°C for 8 h. Unbound proteins were recovered with a magnetic rack. The beads were washed with 20 mM Hepes, pH 7.8, 150 mM NaCl, 20 mM imidazole, and 0.25% digitonin, and bound proteins were eluted with the same buffer containing 100 mM EDTA for 1 h with end-over-end mixing at 4°C. A second elution was performed with 2× SDS buffer containing 100 mM EDTA at room temperature for 1 h. Elution fractions were combined for analysis.

Image acquisition and processing

Images of radiolabeled proteins on polyacrylamide gels and of immunoblots were obtained by digital scanning of fluorogram films and immunoblot films with a scanner (Perfection 3170). Images were analyzed without additional processing and were prepared for figures without or with minimal adjustments of brightness and/or contrast.

Online supplemental material

Fig. S1 shows quantification of IVT radiolabeled proteins and endogenous cpTat components. Fig. S2 shows differential immunoblotting behavior between soluble domain antigens and full-length proteins. Fig. S3 shows a binding saturation assay and Hill slope analysis. Table S1 shows extraction efficiencies of radiolabeled proteins from dried gels. Table S2 shows dual-radiolabel immunoblot calibration. Online supplemental material is available at http://www.jcb.org/cgi/content/full/jcb.201201096/DC1.

The authors thank Cassie Aldridge, Mike McCaffery, and Xianyue Ma for critical review of the manuscript. We also thank Steve Theg for helpful discussions on the kinetics.

This work was supported in part by National Institutes of Health grant R01 GM46951 to K. Cline and a Fulbright-Conicyt grant to J.M. Celedon.

The authors declare that they have no conflict of interests regarding the work reported in this manuscript.

Submitted: 17 January 2012
Accepted: 12 April 2012

References

Alami, M., I. Lüke, S. Deitermann, G. Eisner, H.-G. Koch, J. Brunner, and M. Müller. 2003. Differential interactions between a twin-arginine signal peptide and its translocase in *Escherichia coli*. *Mol. Cell.* 12:937–946. http://dx.doi.org/10.1016/S1097-2765(03)00398-8

Alder, N.N., and S.M. Theg. 2003. Protein transport via the cpTat pathway displays cooperativity and is stimulated by transport-incompetent substrate. *FEBS Lett.* 540:96–100. http://dx.doi.org/10.1016/S0014-5793(03)00231-X

Arnon, D.I. 1949. Copper enzymes in isolated chloroplasts. Polyphenoloxidase in *Beta Vulgaris*. *Plant Physiol.* 24:1–15. http://dx.doi.org/10.1104/pp.24.1.1

Auer, S., and D. Kashchiev. 2010. Insight into the correlation between lag time and aggregation rate in the kinetics of protein aggregation. *Proteins*. 78:2412–2416.

Bageshwar, U.K., N. Whitaker, F.-C. Liang, and S.M. Musser. 2009. Interconvertibility of lipid- and translocon-bound forms of the bacterial Tat precursor pre-SufI. *Mol. Microbiol.* 74:209–226. http://dx.doi.org/10.1111/j.1365-2958.2009.06862.x

Berks, B.C., F. Sargent, and T. Palmer. 2000. The Tat protein export pathway. *Mol. Microbiol.* 35:260–274. http://dx.doi.org/10.1046/j.1365-2958.2000.01719.x

Bolhuis, A., J.E. Mathers, J.D. Thomas, C.M.L. Barrett, and C. Robinson. 2001. TatB and TatC form a functional and structural unit of the twin-arginine translocase from *Escherichia coli*. *J. Biol. Chem.* 276:20213–20219. http://dx.doi.org/10.1074/jbc.M100682200

Brüser, T., and C. Sanders. 2003. An alternative model of the twin arginine translocation system. *Microbiol. Res.* 158:7–17. http://dx.doi.org/10.1078/0944-5013-00176

Chen, Q., L.M. Lauzon, A.E. DeRocher, and E. Vierling. 1990. Accumulation, stability, and localization of a major chloroplast heat-shock protein. *J. Cell Biol.* 110:1873–1883. http://dx.doi.org/10.1083/jcb.110.6.1873

Cline, K. 1986. Import of proteins into chloroplasts. Membrane integration of a thylakoid precursor protein reconstituted in chloroplast lysates. *J. Biol. Chem.* 261:14804–14810.

Cline, K., and H. Mori. 2001. Thylakoid ΔpH-dependent precursor proteins bind to a cpTatC–Hcf106 complex before Tha4-dependent transport. *J. Cell Biol.* 154:719–729. http://dx.doi.org/10.1083/jcb.200105149

Cline, K., and S.M. Theg. 2007. The Sec and Tat Protein Translocation Pathways in Chloroplasts. *In* The Enzymes: Molecular Machines Involved in Protein Transport across Cellular Membranes. Vol. 25. R.E. Dalbey, C.M. Koehler, and F. Tamanoi, editors. Elsevier, London. 463–492.

Cline, K., R. Henry, C. Li, and J. Yuan. 1993. Multiple pathways for protein transport into or across the thylakoid membrane. *EMBO J.* 12:4105–4114.

Connors, K.A. 1990. Chemical Kinetics: The Study of Reaction Rates in Solution. Wiley-VCH, New York. 496 pp.

Dabney-Smith, C., and K. Cline. 2009. Clustering of C-terminal stromal domains of Tha4 homo-oligomers during translocation by the Tat protein transport system. *Mol. Biol. Cell.* 20:2060–2069. http://dx.doi.org/10.1091/mbc.E08-12-1189

Dabney-Smith, C., H. Mori, and K. Cline. 2003. Requirement of a Tha4-conserved transmembrane glutamate in thylakoid Tat translocase assembly revealed by biochemical complementation. *J. Biol. Chem.* 278:43027–43033. http://dx.doi.org/10.1074/jbc.M307923200

Dorne, A.J., J. Joyard, and R. Douce. 1990. Do thylakoids really contain phosphatidylcholine? *Proc. Natl. Acad. Sci. USA*. 87:71–74. http://dx.doi.org/10.1073/pnas.87.1.71

Douce, R., and J. Joyard. 1982. Purification of the Chloroplast Envelope. *In* Methods in Chloroplast Molecular Biology. M. Edelman, N.-H., and R.B. Hallick, editors. Elsevier, Amsterdam. 239–256.

Fincher, V., C. Dabney-Smith, and K. Cline. 2003. Functional assembly of thylakoid deltapH-dependent/Tat protein transport pathway components in

vitro. *Eur. J. Biochem.* 270:4930–4941. http://dx.doi.org/10.1046/j.1432-1033.2003.03894.x

Frielingsdorf, S., M. Jakob, and R.B. Klösgen. 2008. A stromal pool of TatA promotes Tat-dependent protein transport across the thylakoid membrane. *J. Biol. Chem.* 283:33838–33845. http://dx.doi.org/10.1074/jbc.M806334200

Fröbel, J., P. Rose, and M. Müller. 2011. Twin-arginine translocation: Early contacts between substrate proteins and TatA. *J. Biol. Chem.* 286:43679–43689. http://dx.doi.org/10.1074/jbc.M111.292565

Gérard, F., and K. Cline. 2006. Efficient twin arginine translocation (Tat) pathway transport of a precursor protein covalently anchored to its initial cpTatC binding site. *J. Biol. Chem.* 281:6130–6135. http://dx.doi.org/10.1074/jbc.M512733200

Gérard, F., and K. Cline. 2007. The thylakoid proton gradient promotes an advanced stage of signal peptide binding deep within the Tat pathway receptor complex. *J. Biol. Chem.* 282:5263–5272. http://dx.doi.org/10.1074/jbc.M610337200

Gettens, R.T.T., and J.L. Gilbert. 2007. Quantification of fibrinogen adsorption onto 316L stainless steel. *J. Biomed. Mater. Res. A*. 81:465–473.

Gohlke, U., L. Pullan, C.A. McDevitt, I. Porcelli, E. de Leeuw, T. Palmer, H.R. Saibil, and B.C. Berks. 2005. The TatA component of the twin-arginine protein transport system forms channel complexes of variable diameter. *Proc. Natl. Acad. Sci. USA*. 102:10482–10486. http://dx.doi.org/10.1073/pnas.0503558102

Hashimoto, A., W.F. Ettinger, Y. Yamamoto, and S.M. Theg. 1997. Assembly of newly imported oxygen-evolving complex subunits in isolated chloroplasts: Sites of assembly and mechanism of binding. *Plant Cell*. 9:441–452. http://dx.doi.org/10.1105/tpc.9.3.441

Heuberger, E.H.M.L., L.M. Veenhoff, R.H. Duurkens, R.H.E. Friesen, and B. Poolman. 2002. Oligomeric state of membrane transport proteins analyzed with blue native electrophoresis and analytical ultracentrifugation. *J. Mol. Biol.* 317:591–600. http://dx.doi.org/10.1006/jmbi.2002.5416

Hou, B., S. Frielingsdorf, and R.B. Klösgen. 2006. Unassisted membrane insertion as the initial step in DeltapH/Tat-dependent protein transport. *J. Mol. Biol.* 355:957–967. http://dx.doi.org/10.1016/j.jmb.2005.11.029

Jakob, M., S. Kaiser, M. Gutensohn, P. Hanner, and R.B. Klösgen. 2009. Tat subunit stoichiometry in *Arabidopsis thaliana* challenges the proposed function of TatA as the translocation pore. *Biochim. Biophys. Acta*. 1793:388–394. http://dx.doi.org/10.1016/j.bbamcr.2008.09.006

Leake, M.C., N.P. Greene, R.M. Godun, T. Granjon, G. Buchanan, S. Chen, R.M. Berry, T. Palmer, and B.C. Berks. 2008. Variable stoichiometry of the TatA component of the twin-arginine protein transport system observed by in vivo single-molecule imaging. *Proc. Natl. Acad. Sci. USA*. 105:15376–15381. http://dx.doi.org/10.1073/pnas.0806338105

Lee, P.A., D. Tullman-Ercek, and G. Georgiou. 2006. The bacterial twin-arginine translocation pathway. *Annu. Rev. Microbiol.* 60:373–395. http://dx.doi.org/10.1146/annurev.micro.60.080805.142212

Ma, X., and K. Cline. 2000. Precursors bind to specific sites on thylakoid membranes prior to transport on the delta pH protein translocation system. *J. Biol. Chem.* 275:10016–10022. http://dx.doi.org/10.1074/jbc.275.14.10016

Ma, X., and J. Browse. 2006. Altered rates of protein transport in *Arabidopsis* mutants deficient in chloroplast membrane unsaturation. *Phytochemistry*. 67:1629–1636. http://dx.doi.org/10.1016/j.phytochem.2006.04.008

Ma, X., and K. Cline. 2010. Multiple precursor proteins bind individual Tat receptor complexes and are collectively transported. *EMBO J.* 29:1477–1488. http://dx.doi.org/10.1038/emboj.2010.44

Maurer, C., S. Panahandeh, A.-C. Jungkamp, M. Moser, and M. Müller. 2010. TatB functions as an oligomeric binding site for folded Tat precursor proteins. *Mol. Biol. Cell*. 21:4151–4161. http://dx.doi.org/10.1091/mbc.E10-07-0585

McDevitt, C.A., G. Buchanan, F. Sargent, T. Palmer, and B.C. Berks. 2006. Subunit composition and in vivo substrate-binding characteristics of *Escherichia coli* Tat protein complexes expressed at native levels. *FEBS J.* 273:5656–5668. http://dx.doi.org/10.1111/j.1742-4658.2006.05554.x

Mori, H., and K. Cline. 2002. A twin arginine signal peptide and the pH gradient trigger reversible assembly of the thylakoid ΔpH/Tat translocase. *J. Cell Biol.* 157:205–210. http://dx.doi.org/10.1083/jcb.200202048

Mori, H., E.J. Summer, X. Ma, and K. Cline. 1999. Component specificity for the thylakoidal Sec and Delta pH–dependent protein transport pathways. *J. Cell Biol.* 146:45–56.

Mori, H., E.J. Summer, and K. Cline. 2001. Chloroplast TatC plays a direct role in thylakoid (Δ)pH-dependent protein transport. *FEBS Lett.* 501:65–68. http://dx.doi.org/10.1016/S0014-5793(01)02626-6

Müller, M., and R.B. Klösgen. 2005. The Tat pathway in bacteria and chloroplasts (review). *Mol. Membr. Biol.* 22:113–121. http://dx.doi.org/10.1080/09687860500041809

Musser, S.M., and S.M. Theg. 2000. Characterization of the early steps of OE17 precursor transport by the thylakoid DeltapH/Tat machinery. *Eur. J. Biochem.* 267:2588–2598. http://dx.doi.org/10.1046/j.1432-1327.2000.01269.x

Orriss, G.L., M.J. Tarry, B. Ize, F. Sargent, S.M. Lea, T. Palmer, and B.C. Berks. 2007. TatBC, TatB, and TatC form structurally autonomous units within the twin arginine protein transport system of *Escherichia coli*. *FEBS Lett.* 581:4091–4097. http://dx.doi.org/10.1016/j.febslet.2007.07.044

Panahandeh, S., C. Maurer, M. Moser, M.P. DeLisa, and M. Müller. 2008. Following the path of a twin-arginine precursor along the TatABC translocase of *Escherichia coli*. *J. Biol. Chem.* 283:33267–33275. http://dx.doi.org/10.1074/jbc.M804225200

Patrick, T.D., C.E. Lewer, and V.M. Pain. 1989. Preparation and characterization of cell-free protein synthesis systems from oocytes and eggs of *Xenopus laevis*. *Development*. 106:1–9.

Reed, J.E., K. Cline, L.C. Stephens, K.O. Bacot, and P.V. Viitanen. 1990. Early events in the import/assembly pathway of an integral thylakoid protein. *Eur. J. Biochem.* 194:33–42. http://dx.doi.org/10.1111/j.1432-1033.1990.tb19423.x

Rodrigue, A., A. Chanal, K. Beck, M. Müller, and L.F. Wu. 1999. Co-translocation of a periplasmic enzyme complex by a hitchhiker mechanism through the bacterial tat pathway. *J. Biol. Chem.* 274:13223–13228. http://dx.doi.org/10.1074/jbc.274.19.13223

Sargent, F., B.C. Berks, and T. Palmer. 2006. Pathfinders and trailblazers: A prokaryotic targeting system for transport of folded proteins. *FEMS Microbiol. Lett.* 254:198–207. http://dx.doi.org/10.1111/j.1574-6968.2005.00049.x

Stanley, N.R., T. Palmer, and B.C. Berks. 2000. The twin arginine consensus motif of Tat signal peptides is involved in Sec-independent protein targeting in *Escherichia coli*. *J. Biol. Chem.* 275:11591–11596. http://dx.doi.org/10.1074/jbc.275.16.11591

Summer, E.J., H. Mori, A.M. Settles, and K. Cline. 2000. The thylakoid delta pH-dependent pathway machinery facilitates RR-independent N-tail protein integration. *J. Biol. Chem.* 275:23483–23490. http://dx.doi.org/10.1074/jbc.M004137200

Tarry, M.J., E. Schäfer, S. Chen, G. Buchanan, N.P. Greene, S.M. Lea, T. Palmer, H.R. Saibil, and B.C. Berks. 2009. Structural analysis of substrate binding by the TatBC component of the twin-arginine protein transport system. *Proc. Natl. Acad. Sci. USA*. 106:13284–13289. http://dx.doi.org/10.1073/pnas.0901566106

Tossi, A., L. Sandri, and A. Giangaspero. 2000. Amphipathic, α-helical antimicrobial peptides. *Biopolymers*. 55:4–30. http://dx.doi.org/10.1002/1097-0282(2000)55:1<4::AID-BIP30>3.0.CO;2-M

Weimer, P.J., J.M. Lopez-Guisa, and A.D. French. 1990. Effect of cellulose fine structure on kinetics of its digestion by mixed ruminal microorganisms in vitro. *Appl. Environ. Microbiol.* 56:2421–2429.

Whitaker, N., U.K. Bageshwar, and S.M. Musser. 2012. Kinetics of precursor interactions with the bacterial Tat translocase detected by real-time FRET. *J. Biol. Chem.* In Press.

Celedon and Cline, http://www.jcb.org/cgi/content/full/jcb.201201096/DC1

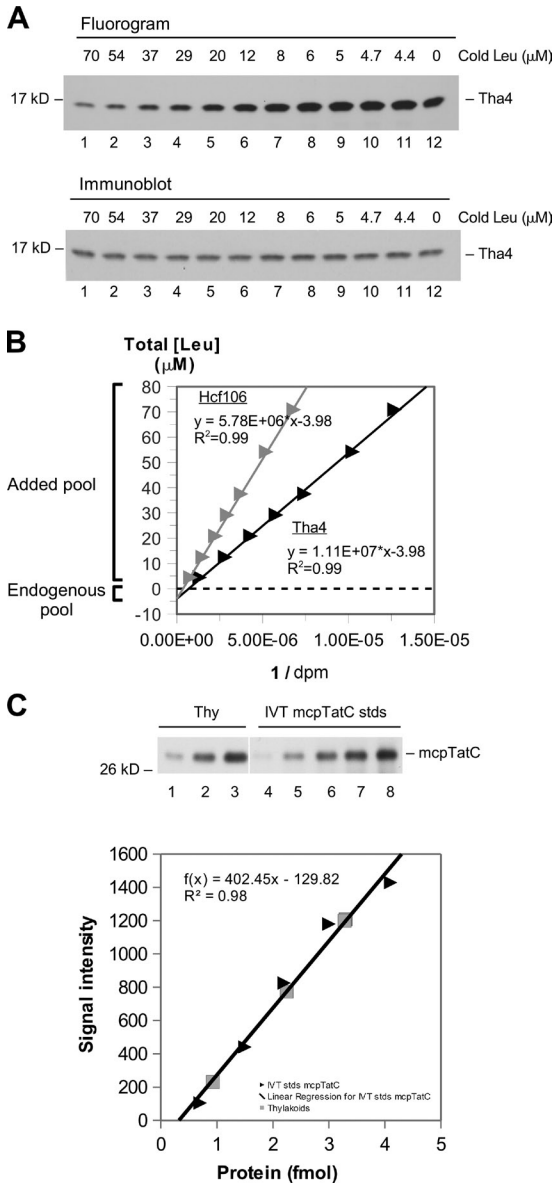

Figure S1. **Quantification of IVT radiolabeled proteins and endogenous cpTat components.** (A) Isotope dilution analysis to determine the Leu-specific radioactivity in the translation reaction. WG translation reactions programmed with mRNA for Tha4, Hcf106, or cpTatC and containing a fixed amount of ^{3}H-Leu and increasing amounts of unlabeled Leu were incubated at 25°C for 1 h and analyzed by SDS-PAGE followed by fluorography and immunoblotting. Immunoblotting band intensities indicated that Leu was not limiting in any translation reaction. (B) Radiolabeled translation products were extracted from gel slices, and dpm were determined by scintillation counting (see Materials and methods). The concentration of total known Leu added to the reactions (added unlabeled Leu plus added ^{3}H-Leu) was plotted versus the reciprocal of the radioactivity. The size of the endogenous pool of unlabeled amino acid corresponds to the negative intercept of the regression line with the y axis according to the equation $y = m \times 1/dpm + c$, where y is the added unlabeled Leu plus added ^{3}H-Leu, m is the slope of the regression line, and c the intercept with the y axis. Three different mRNAs were used for each isotope dilution experiment. Tha4 and Hcf106 are shown. (C) Immunoblot quantification of cpTatC using IVT cpTatC as standards (IVT mcpTatC stds). IVT mcpTatC was quantified by SDS-PAGE/fluorography and scintillation counting as in B. Thylakoid (Thy) membranes and the IVT mcpTatC were subjected to immunoblotting analysis, as described in Materials and methods. Densitometry analysis within the linear range of standards was used to estimate the concentration of thylakoid cpTatC. The data plotted in B are representative of data obtained for each WG translation extract used in this study, and the immunoblotting calibration curve in C is representative of calibration curves produced for each cpTat component quantification.

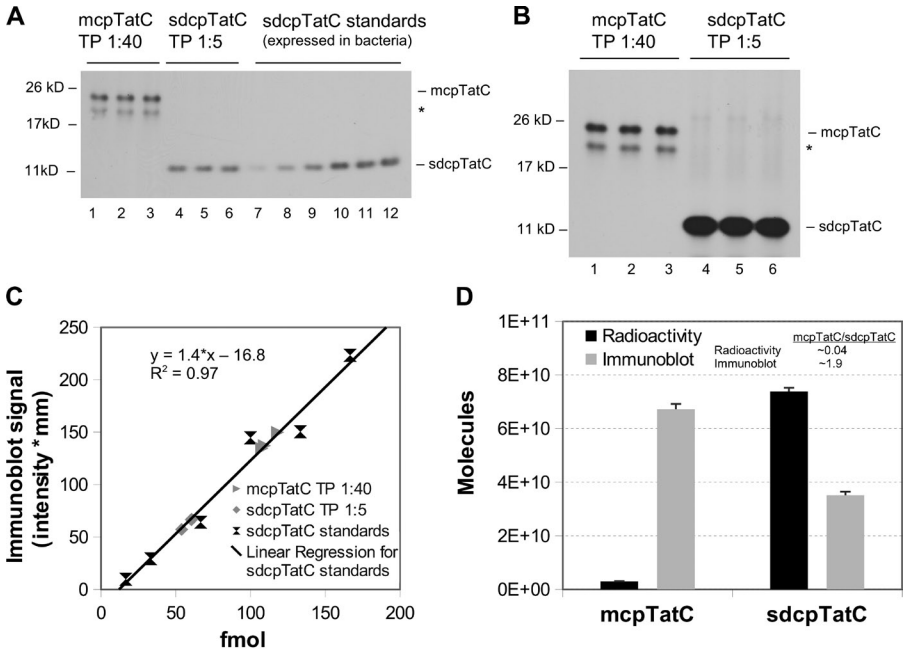

Figure S2. **Differential immunoblotting behavior between soluble domain antigens and full-length proteins.** (A and B) Full-length cpTatC (mcpTatC) and stromal domain cpTatC (sdcpTatC) were IVT and diluted to give similar immunoblot signal intensities. Antibodies generated against sdcpTatC were used for immunoblotting. Samples were loaded in triplicate and analyzed by 10% tricine SDS-PAGE followed by immunoblotting (A) or fluorography (B). Electroblotting and detection were performed as described in Materials and methods. TP, translation product. (C) Immunoblot quantification by densitometry analysis was performed within the linear range of sdcpTatC standards of known concentration expressed in bacteria. Proteins were quantified by scintillation counting, as described in Materials and methods. (A–C) Asterisks denote the degradation product of mcpTatC not considered in quantifications. (D) Comparison of the amounts of protein quantified by scintillation counting versus immunoblotting. The data correspond to three independent replicates (n = 3). Error bars represent SD.

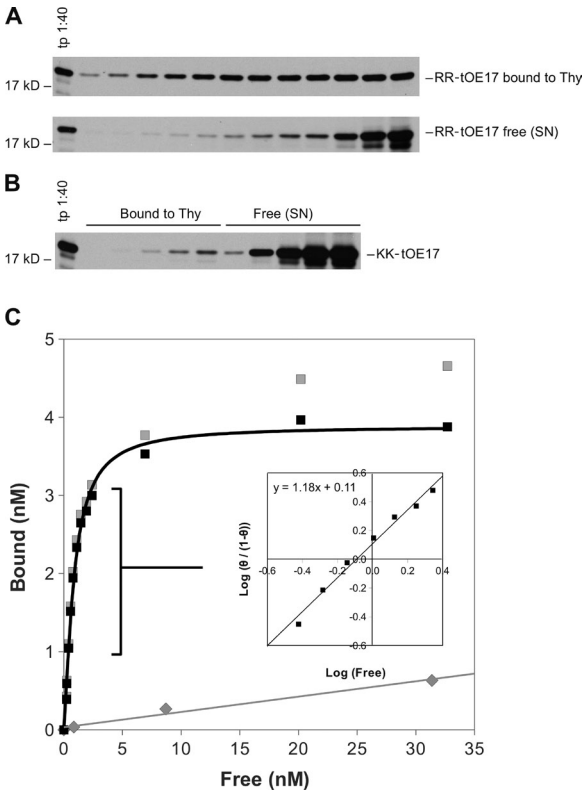

Figure S3. **Binding saturation assay and Hill slope analysis.** (A) Increasing amounts of radiolabeled RR-tOE17 were incubated with washed thylakoids (Thy) for 1 h at 4°C in a binding reaction. The amounts of precursor protein in binding reactions were chosen to increase the number of data points in the middle region of the binding isotherm. Membranes were recovered by centrifugation and washed twice with IBM. Samples were analyzed by SDS-PAGE and fluorography, and the precursor was recovered with thylakoids (top) and in the supernatant (SN; bottom), quantified by scintillation counting of extracted gel bands. tp, translation product. (B) Nonspecific binding was estimated in a parallel binding assay with a nonfunctional KK-tOE17. (C) Total bound precursor (gray squares), nonspecific binding (gray diamonds and line), and total specific binding (i.e., total minus nonspecific binding; black squares and line) were plotted versus free unbound precursor and fit to a single binding site model. The data in the rising region of specific binding, as indicated, were used for the Hill plot (inset; as described in Materials and methods). The data are from a single experiment, with an emphasis on data points in the middle region of the binding curve. Hill coefficients were also determined for four additional experiments.

Table S1. **Extraction efficiencies of radiolabeled proteins from dried gels**

Protein	In solution[a]	Gel extracted[b]								Correction factors[f]	
	Ni^{++} purified or membrane associated	Main band[b]		Above main band[c]		Below main band[d]		Total radioactivity extracted[e]		IVT stds[g]	Membrane-associated proteins[h]
		Ni^{++} purified	Membrane associated	Ni^{++} purified	Membrane associated	Ni^{++} purified	Membrane associated	Ni^{++} purified	Membrane associated		
	%	%	%	%	%	%	%	%	%		
cpTatC	100	60 (0.6)	67 (1.3)	19 (0.5)	11 (0.2)	14 (0.8)	8 (0.2)	94 (0.7)	86 (2.9)	1.06	1.36
Hcf106	100	72 (0.4)	73 (0.1)	3 (0.2)	3 (0.03)	15 (0.3)	9 (0.01)	90 (0.7)	85 (0.1)	1.11	1.23
Tha4	100	71 (1.0)	79 (1.5)	9 (0.7)	7 (0.3)	5 (0.2)	5 (0.1)	85 (1.6)	91 (1.2)	1.18	1.20
tOE17	100	89 (0.5)	82 (0.6)	1 (0.1)	3 (0.3)	5 (0.04)	5 (0.1)	95 (0.6)	90 (0.7)	NA	1.15

All numbers reported are means of three technical replicates. SDs are indicated in parentheses.
[a]IVT proteins were purified by metal ion affinity chromatography (Ni^{++}) or by incorporation into thylakoid membranes by chloroplast import (cpTatC), thylakoid integration (Hcf106 and Tha4), or binding (tOE17) followed by SDS solubilization of membranes, as described in Materials and methods. The proteins purified in solution were directly quantified by scintillation counting and represent 100% of radiolabel loaded to gel lanes.
[b]Purified proteins in SDS-PAGE gel slices were extracted and counted (see Materials and methods). Percentages of recoveries are gel-extracted dpm divided by in-solution dpm × 100.
[c]The SDS gel above the main translation product band. This contains protein aggregates apparent with long film exposure.
[d]The SDS gel below the main band.
[e]The total radioactivity recovered from SDS-PAGE fluorogram gel lanes. This was used to determine the extraction efficiency correction factor.
[f]Extraction efficiency correction factors used to correct for recovery of radiolabel from gels (i.e., dpm × correction factor).
[g]Correction factors for quantification of IVT standards (stds) were 100 divided by the total percentage of radioactivity extracted, using Ni^{++}-purified protein extraction data.
[h]Correction factors for quantification of membrane-associated Tat components and bound precursor protein were calculated as 100 × (percentage of main band + percentage above main band)/(percentage of main band × percentage of total radioactivity extracted) using the membrane-associated extraction data.

Table S2. **Dual-radiolabel immunoblot calibration**

Protein	Immunoblot quantification			Radiolabel quantification[d]	R/I[e]	Correction factor[f]
	Mock[a]	Import or integration[b]	Immunoblot estimation of imported/integrated[c]	Imported or integrated		
	molecule/Thy	*molecule/Thy*	*molecule/Thy*	*molecule/Thy*		
cpTatC	6,600 (1,300)	8,600 (1,700)	2,000 (900)	2,500 (1,100)	1.25	1.45
Hcf106	33,600 (8,300)	87,500 (20,100)	53,900 (12,100)	60,700 (1,500)	1.13	1.17
Tha4	55,200 (10,200)	150,700 (15,800)	95,500 (7,600)	99,900 (5,800)	1.05	1.14

All numbers reported are means of three technical replicates. SDs are indicated in parentheses. Thy, thylakoid.
[a]Immunoblot quantification of cpTat components in mock-treated thylakoids using IVT full-length radiolabeled standards, as explained in Materials and methods and Fig. S1.
[b]Immunoblot quantification of cpTat components in thylakoids after import/integration of radiolabeled components.
[c]Immunoblot estimate of radiolabeled import/integration components calculated as (import/integration − mock).
[d]Radiolabel quantification of imported/integrated components, as explained in Materials and methods, Fig. S1, and Table S1.
[e]Amount of imported/integrated component quantified by radiolabel divided by the amount quantified by immunoblotting (R/I).
[f]Correction factor for immunoblot quantification of membrane-associated components to account for proteins in the main band and above the main band. Correction factors are derived from Table S1 and R/I.